High-Density Myoelectric Pattern Recognition Toward Improved Stroke Rehabilitation

Xu Zhang, *Member, IEEE*, and Ping Zhou* , *Senior Member, IEEE*

***Abstract*—Myoelectric pattern-recognition techniques have been developed to infer user's intention of performing different functional movements. Thus electromyogram (EMG) can be used as control signals of assisted devices for people with disabilities. Pattern-recognition-based myoelectric control systems have rarely been designed for stroke survivors. Aiming at developing such a system for improved stroke rehabilitation, this study assessed detection of the affected limb's movement intention using high-density surface EMG recording and pattern-recognition techniques. Surface EMG signals comprised of 89 channels were recorded from 12 hemiparetic stroke subjects while they tried to perform 20 different arm, hand, and finger/thumb movements involving the affected limb. A series of pattern-recognition algorithms were implemented to identify the intended tasks of each stroke subject. High classification accuracies (96.1% ± 4.3%) were achieved, indicating that substantial motor control information can be extracted from paretic muscles of stroke survivors. Such information may potentially facilitate improved stroke rehabilitation.**

***Index Terms*—High-density surface EMG, myoelectic control, pattern recognition, stroke rehabilitation.**

I. Introduction

STROKE is a leading cause of serious, long-term disability in many countries. Approximately 15 million people in the world suffer from stroke each year, among which 5 million people are permanently disabled [1]. The most common disability following stroke is a physical limitation such as weakness or hemiparesis, which diminishes health-related quality of life. Specifically, upper limb (arm, hand, finger/thumb) dexterity is often limited in the contralesional or affected side. It is necessary to improve the restoration of upper limb function, due to its importance in daily activities [2], [3].

A number of mechatronic devices (e.g., the MIT-Manus robot [4], [5] and the MIME robot [6], [7]) have been designed as assistive tools for robot-aided stroke rehabilitation to improve upper limb function [3]–[14]. Most of the devices can assist users to perform exercises which involve repetitive movement of their paretic limb in a passive way (as they relax) [7]–[11], or in an active way (as they intend to contribute to the movement) [11], [12]. Although passive movements have been proved to facilitate brain plasticity with improved upper limb functions [8]–[11], the active or voluntary implementation of tasks with the user's intention input is preferred due to its enhanced therapeutic effect [15]. Such active approach, namely interactive control, might also promote motor learning in stroke survivors [3], [7], [16].

Surface electromyogram (EMG) signals contain rich motor control information, from which the user's intention can be detected. For example, EMG signals from amputees' residual muscles have been used as prosthesis control signals for nearly 40 years [17]. Myoelectric control has also been reported in robot-aided therapy for stroke subjects, primarily based on an "ON–OFF" control strategy. Such studies developed robotic systems operating with a predefined trajectory or action once the system was triggered by EMG signals [11]. Song *et al*. [3] further investigated the use of a proportional control strategy in robot-aided stroke rehabilitation. In their study, the robotic system could enable stroke subjects to perform exercises beyond their initial range of motion with additional continuous assistive torque in proportion to the amplitude of EMG signal. Recently, on the demand for the mobility of assistive devices, exoskeleton or wearable robots [18]–[20] have been developed to be worn by stroke subjects as a powered orthosis, applying assistive torque estimated by EMG signals to the joint to help with the movement of a paretic limb. Such applications are usually designed to map the EMG of a single weak muscle to a single degree-of-freedom (DOF) control.

Due to the upper-limb dexterity, however, most functional tasks are generally accomplished through complex temporal and spatial coordination of multiple muscles. It is unfeasible to realize the control of such multiple DOFs via one-to-one mapping (between a muscle and a DOF). Pattern-recognition techniques have recently attracted increasing attention in the development of myoelectric control systems [17], which operate on the assumption that the features extracted from EMG signals at given electrode placement reflect the inherent activity patterns of multiple muscles [21]. The advancement in EMG feature extraction and pattern-recognition techniques provides a powerful approach for identification of various movements and, furthermore, for control of multiple DOFs.

Although great success has been achieved in myoelectric prosthesis control using novel pattern-recognition techniques, few studies have applied such techniques to stroke survivors with various levels of neuromuscular impairments. In this case,

Manuscript received October 14, 2011; revised February 15, 2012; accepted March 7, 2012. Date of publication March 21, 2012; date of current version May 18, 2012. This work was supported in part by the National Institutes of Health under Grant 2R24HD050821. *Asterisk indicates corresponding author*.

X. Zhang is with the Sensory Motor Performance Program, Rehabilitation Institute of Chicago (RIC), Chicago, IL 60611 USA (e-mail: xzhang@ric.org).

*P. Zhou is with the Sensory Motor Performance Program, Rehabilitation Institute of Chicago, Chicago, IL 60611 USA, with the Department of Physical Medicine and Rehabilitation, Northwestern University, Chicago, IL 60611 USA, and also with the Institute of Biomedical Engineering, University of Science and Technology of China, Hefei, 230027 China (e-mail: p-zhou@northwestern.edu).

Digital Object Identifier 10.1109/TBME.2012.2191551

the assessment of the motor control information remaining in the affected limb (i.e., detection of affected limb's movement intention) is of great importance for building myoelectric control systems toward improved stroke rehabilitation. A previous study [2] assessed classification of six intended hand functions of stroke subjects with untargeted placement of ten surface electrodes on forearm and hand muscles, and achieved the mean classification accuracy of 71.3% for moderately impaired subjects and 37.9% for severely impaired subjects.

In this study, novel high-density surface EMG methods were used to examine whether a series of arm, hand, and finger/thumb movement intentions of stroke survivors can be reliably identified. We hypothesize that high accuracies can be achieved in classification of these movement intentions through high-density EMG recording and pattern-recognition analyses. Furthermore, it is possible to maintain high levels of classification accuracy by selecting a limited number of electrodes from such high-density EMG recordings. In this regard, high-density EMG provides important guidance for optimizing electrode number and location to detect the intended movements. The intention of these movements, if detectable, can be used to trigger a movement assistive device (e.g., an EMG-driven exoskeleton robot) for voluntary exercise or rehabilitation training [13], [18]–[20]. Compared with the involuntary or forced exercise, voluntary input has been shown to be the more effective intervention for facilitating motor recovery after stroke [14], [22].

This rest of the paper is organized in three sections. The next section describes the methods of high-density surface EMG recording and myoelectric pattern recognition. Section III describes the experimental results, followed by the discussions and the conclusions in Section IV.

II. Methods

A. Subjects

Twelve post-stroke subjects (eight males, four females, 61 ± 10 years) participated in this study. The study was approved by the Institutional Review Board of Northwestern University (Chicago, IL, USA). All our stroke subjects were recruited from the Clinical Neuroscience Research Registry at the Rehabilitation Institute of Chicago (Chicago, IL, USA), and all subjects gave their written consent before the experiment. A screening examination and clinical assessment to determine the eligibility for each stroke subject were performed by a physical therapist. Inclusion criteria for participation of the study include: 1) age between 21–85 years old; 2) experience of stroke, initial onset $>$6 months; 3) medically stable with clearance to participate; 4) ability to provide informed consent, with Minimental state examination must be 25 or higher; 5) first time stroke. Exclusion criteria include: 1) history of spinal cord injury or traumatic brain damage; 2) inability to maintain 2 h of participation in data collection due to any reason; 3) inability to comprehend conversations; 4) history of serious medical illness such as cardiovascular or pulmonary complications; 5) history of severe motion sickness; 6) any condition that, in the judgment of a physician, would prevent the person from participating. Women who are pregnant or nursing were excluded from the study. There was no requirement for stroke subjects to be able to perform the tested movements using the affected limb. All the 12 subjects were right-handed before stroke. Demographic and clinical measures [23], [24] for the stroke subjects are detailed in Table I.

TABLE I
Physical Characteristics of Subjects

Subject #	Age	Sex	Duration	Paretic	F-M (U-L)	C-M Hand
1	59	F	13	L	28	2
2	56	M	23	L	15	2
3	67	M	8	L	20	4
4	63	F	7	R	19	2
5	45	M	6	L	58	5
6	58	F	2	R	23	2
7	64	M	8	L	38	2
8	61	M	7	R	56	4
9	65	M	15	L	20	2
10	46	M	13	L	52	3
11	81	M	17	L	28	2
12	71	F	22	R	22	3

Duration: years since the onset of stroke. Paretic: the side of hemiparesis. F-M (U-L): the Fugl–Meyer assessment scale of the paretic upper-limb (total score: 66) [23]. C-M Hand: the hand impairment part of the Chedoke–McMaster stroke assessment scale (from 1 to 7) [24].

B. Data Acquisition

High-density surface EMG signals consisting of 89 channels were collected from the upper arm, forearm and hand muscles in the affected side of each stroke subject. A Refa128 EMG system (TMS International BV, Enschede, Netherlands) was used for the recording.

Fig. 1 illustrates the placement of the electrodes, using the left arm as an example. To facilitate electrode placement, the 89 electrodes were arranged in three different groups [see Fig. 1(a)]. A detailed description of the electrode positions is presented in Fig. 1(b). Since both the upper arm and the forearm can be approximately considered as cylinders, 80 electrodes were arranged in a grid formation with ten round groups labeled with uppercase letters from "A" to "J", and eight lateral groups labeled with lowercase letters from "a" to "h". The round groups labeled from "A" to "D" were placed on the upper arm at a location from 37.5% to 75% for every 12.5% of the entire distance from the greater tubercle of the humerus to the medial epicondyle of the humerus, respectively.

Similarly on the forearm, the round groups labeled from "E" to "J" were placed at a location from 12.5% to 75% for every 12.5% of the entire distance from the medial epicondyle of the humerus to the styloid process of the ulna, respectively. In each round group, eight electrodes were equally spaced around the circumference of the arm, and each of them also belonged to a different lateral group, as shown in Fig. 1(c). The electrodes in lateral group "a" were placed in a line along the center of the posterior side of the upper arm or forearm, whereas the lateral group "e" was along the center of the anterior side.

On the hand, the remaining nine electrodes were divided into three groups (with three electrodes for each group), which were

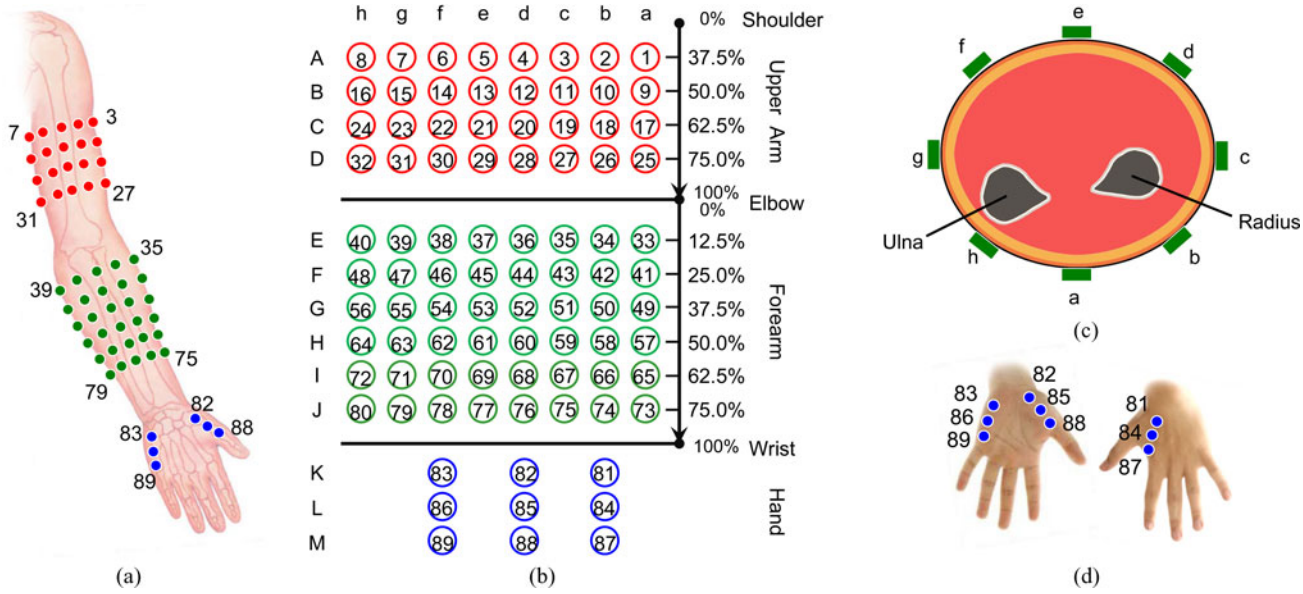

Fig. 1. Electrode placement for 89-channel EMG signal recordings. (a) Schematic diagram of electrode placement with numbers indicating the index of EMG channel. Only the electrode positions on the anterior aspect of the upper arm, forearm, and hand are visible. (b) Electrode arrangement in a grid formation with ten round groups and eight lateral line groups. The open circles with channel index number inside represent the surface EMG electrodes. (c) Cross section of forearm through round group H, which is located in the middle of the forearm. (d) The positions of nine electrodes on three hand muscles.

placed on the first dorsal interosseous (FDI), thenar group and hypothenar group muscles, as shown in Fig. 1(d).

The size of each individual electrode was 10 mm in diameter, while the recording surface was 5 mm in diameter. After the recording surface was filled with conductive gel using a syringe, the electrode was then attached to the skin using a double-sided adhesive disc. The center-to-center distance between two consecutive electrodes depends on the size of the arm. Generally, the distance between two round groups was approximately 10 mm, and the distance between two lateral groups was approximately 15 mm. The surface EMG signals were sampled at 2000 Hz per channel. All the 89 channels of surface EMG signals were able to be continuously monitored during the experiment.

TABLE II
LIST OF THE FUNCTIONAL MOVEMENTS

Index	Movement	Index	Movement
1	Wrist Flexion	2	Wrist Extension
3	Wrist Supination	4	Wrist Pronation
5	Elbow Flexion	6	Elbow Extension
7	Hand Open	8	Hand Close
9	Thumb Extension	10	Thumb Flexion
11	Index Finger Flexion	12	Index Finger Extension
13	Fingers 3-5 Flexion	14	Fingers 3-5 Extension
15	Fine Pinch	16	Lateral Pinch
17	Tip Pinch	18	Gun Posture
19	Ulnar Wrist Down	20	Ulnar Wrist Up

C. Experimental Protocol

Each stroke subject was comfortably seated in a chair with the affected upper limb relaxed on a height-adjustable table. The subject was instructed to perform 20 different functional movements as listed in Table II. During the experiment, a video of each movement performed by a healthy individual was used as demonstration for guiding the stroke subject to perform (or more accurately, intend to perform) each movement.

The experiment comprised of 20 trials. Each experimental trial contained five repetitions of one movement. For each repetition of a movement, the subject was instructed to perform the task with a moderate or comfortable force, hold the task for 3 s and then relax for approximately 10 s between repetitions. Additional relax time between repetitions of each task was allowed to help the stroke subjects decrease muscle spasticity or involuntary EMG activity before performing the next task. The subject was allowed to rest for 3–5 min between trials to avoid muscular and mental fatigue.

D. Data Preprocessing and Segmentation

The collected surface EMG signals were first processed with a fourth-order Butterworth bandpass filter (30–500 Hz) to remove the movement artifacts and high-frequency noises.

For each movement, the recorded EMG data were composed of five active segments corresponding to five repetitions of muscle contraction. A suitable segmentation of contraction/ no contraction epochs was performed manually for each movement. Several signal channels with clear EMG activities and quiescent baseline in between were visually chosen and then averaged as a single data stream, as shown in Fig. 2. Then the onset and offset times of each active segment were manually determined and applied to all the channels [25]–[27]. Ideally, an automatic amplitude-based thresholding algorithm would be used to segment the data. However, in some recording sessions, subjects produced muscle activity on returning from the actuated task to the neutral position. To avoid mislabeling, we used the manual segmentation.

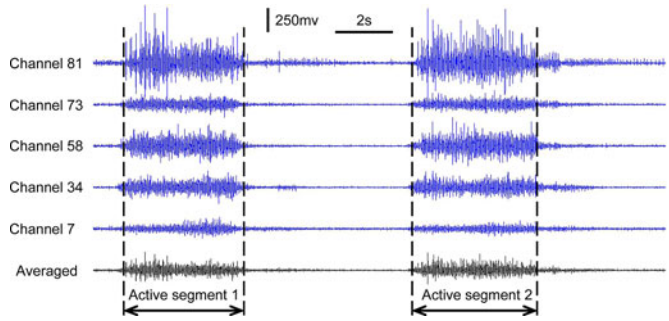

Fig. 2. Surface EMG signals from randomly chosen channels during the movement of hand open with two repetitions. The signals of three channels (81, 58, and 34) were used to calculate the averaged signal stream for data segmentation.

For each active segment, 89-channel EMG data were further segmented into a series of overlapping analysis windows (window length: 256 ms, overlapping step: 128 ms). The following EMG feature extraction and pattern classification methods were then performed on these analysis windows. The overlapped windowing scheme was used to enhance both utilization of limited data stream and continuity of decision output by the classifier.

E. Feature Extraction

For each analysis window, a set of features was extracted to characterize the EMG data for classification of the intended movements. Two feature sets were investigated in this study: the time domain (TD) feature set proposed by Hudgins *et al.* [28] and the combination of autoregressive (AR) model (sixth-order as suggested by Farina and Merletti [29]) coefficients and the rms of the signal as a feature set (AR+RMS). These features have been shown to be effective signal representation for EMG pattern recognition with relatively low computational complexity [17], [28]–[32]. The feature set was computed on each of the 89 EMG channels and then concatenated into a feature vector.

F. Feature Dimensionality Reduction

The high-density surface EMG recording resulted in very high-order n-dimensional feature vectors ($n = 356$ for TD feature set; $n = 623$ for AR+RMS feature set). To reduce feature dimensionality, a combined approach based on principal component analysis (PCA) and linear discriminant analysis (also known as Fisher linear discriminant (FLD) analysis) was used [33]–[35]. First, the original n-dimensional feature vectors were projected to an m-dimensional subspace through the PCA ($m \leq n$). Then the enhanced FLD model (EFM) [33] was performed to choose a set of s-dimensional features ($s \leq m$) by enhancing the separability among different classes, i.e., by deriving an $s \times m$ projection matrix that maximizes the ratio of between-class scatter to within-class scatter. In this study, s was set to C-1 ($C = 20$) and m was determined from examination of the classification performance.

G. Classification

A number of classifiers have proved to be effective for EMG classification [17]. Three classifiers were used in this study, given as follows.

1) Linear discriminant classifier (LDC) based on the maximum *a-posteriori* probability (MAP) rule and Bayesian principles [33], [41], [42].
2) Gaussian mixture model (GMM). The GMM models each class with a Gaussian mixture density instead of a single model of Gaussian distribution used in the LDC [31], [36]–[38]. In this study, we chose the same classifier settings as in [11]: the number of mixture components was assigned as 3; the variance limiting constraint was set to be 0.05, and the GMM with diagonal covariance matrices was applied.
3) Support vector machine (SVM) [39]. The SVM has the advantages in dealing with limited data samples, high-dimensional and nonlinear pattern recognitions. The SVM is a kernel-based approach, which finds a linear separating hyperplane with maximal margin in a higher dimensional feature space, where the training data are mapped using a nonlinear kernel function. In this study, the library for SVMs developed by Chang *et al.* [40] was used to implement the SVM classifiers. The radial basis function (RBF) kernel was chosen to create nonlinear decision boundaries of classifiers.

H. Performance Evaluation and Statistical Analysis

Pattern recognition was performed for each stroke subject. To make efficient use of the collected data, the fivefold cross-validation scheme was used. The EMG data within any four active segments were selected and assigned as training dataset, and sequentially the EMG data of the remaining active segment were referred to as the testing dataset. The accuracy for each test was the percentage of correctly classified windows over all the testing windows including all the movements. For each subject, the performance was evaluated as the averaged accuracy across the fivefolds. An overall performance was then calculated as the mean and standard deviation (SD) of classification accuracies across all the subjects. Paired t-tests were used to compare the pattern-recognition performance using different feature sets (TD and AR+RMS) or classifiers (LDC, GMM and SVM).

I. Channel Selection

A preliminary study was also conducted to assess the pattern-recognition performance using a subset of the EMG channels. The straightforward sequential feedforward selection algorithm was used, which iteratively added the most informative channels in terms of classification accuracy [41], [43].

III. Experimental Results

A. Characterization of Muscle Activity Patterns

The spatial EMG activity for each movement was characterized by contour plots, where the rms value of each channel's

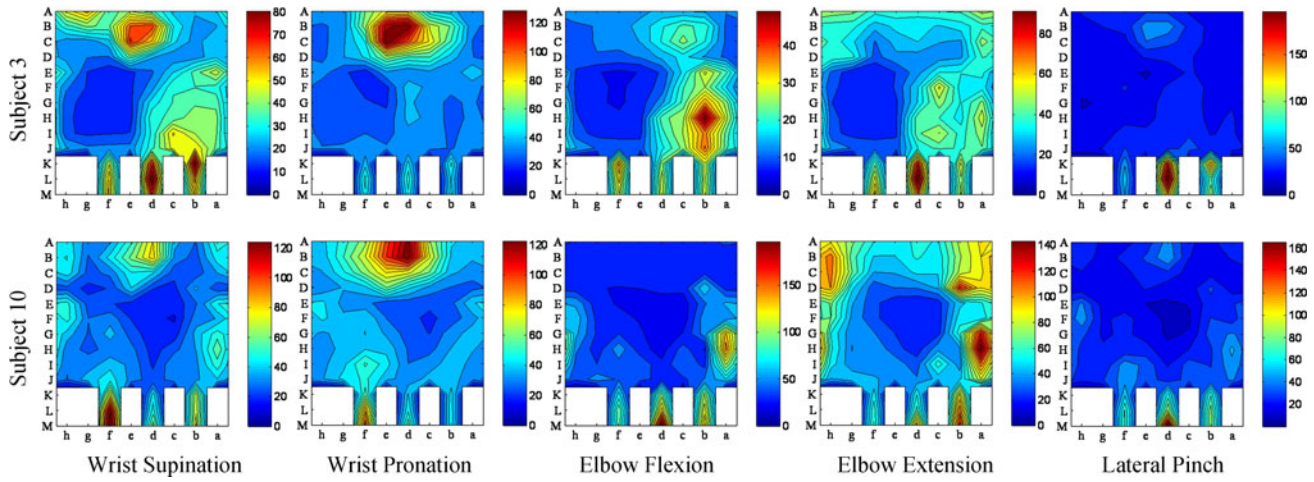

Fig. 3. Examples of the surface EMG amplitude (unit in μV) contour plots for five different movements from two typical subjects (Subject 3 and Subject 10).

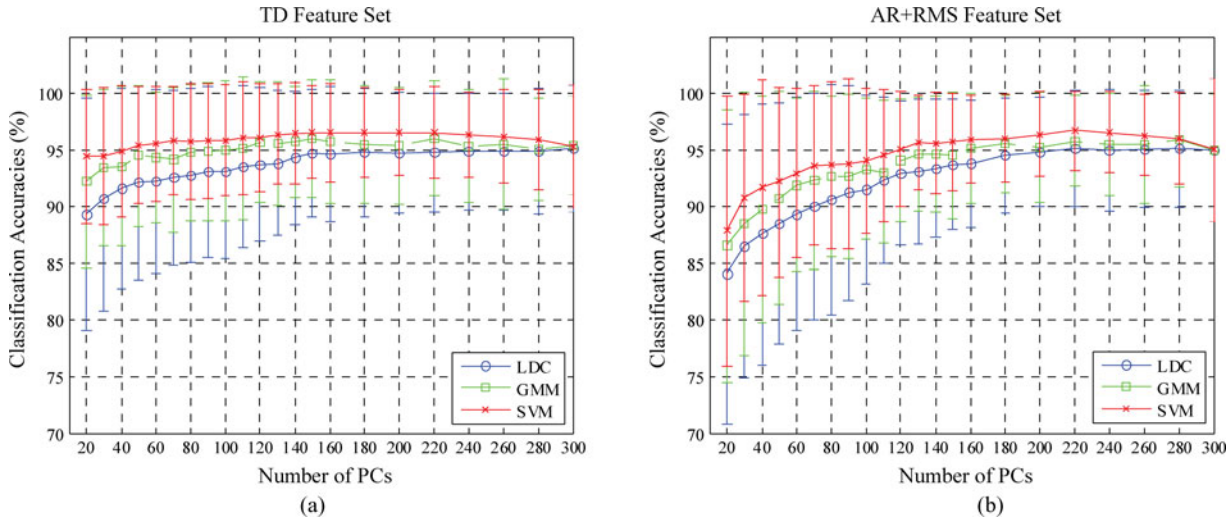

Fig. 4. Effect of number of PCs on the classification performance evaluated by the three classifiers. The classification accuracies are averaged across 12 subjects and plotted with SD error bars. The figures present the results when using (a) the TD feature set, and (b) the AR+RMS feature set.

EMG (averaged over five active segments), was represented by different colors, interpolating the EMG amplitude between electrode sites. With each intended movement, the intensity of the surface EMG signal over the upper limb muscles had a distinct pattern. Fig. 3 shows an example of the spatial EMG activity for five different movements of two subjects. It is worth noting that the contour plots were solely based on EMG amplitude while more features were extracted in the following pattern-recognition analysis.

B. Effect of Number of PCs on Performance

Fig. 4 shows the effect of the number of PCs on the classification performance when using different feature sets and classifiers. With the TD feature set, as shown in Fig. 4(a), the accuracies for all three classifiers steadily increased to relatively high values (about 96%) approximately from 20 to 150 (0.29 $\pm$ 0.12%/10 PCs, averaged across three classifiers) and kept almost constant over the number of PCs up to 220 (0.03 $\pm$ 0.03%/10 PCs). However, when using more PCs (>220), the classification accuracies did not show clear improvement (0.02 $\pm$ 0.03%/10 PCs), and even slightly decreased for GMM ($-$0.08%/10 PCs) and SVM ($-$0.15%/10 PCs) classifiers. Fig. 4(b) shows a similar trend with the AR+RMS feature set. The accuracies for all the classifiers improved to high values with the number of PCs less than 220 (0.57 $\pm$ 0.07%/10 PCs) and then decreased slightly when the number of PCs was more than 220 ($-0.11 \pm 0.09\%$ /10 PCs). Therefore, the optimal number of PCs was chosen as $m = 150$ for the TD feature set and $m = 220$ for the AR+RMS feature set. This number of PCs can effectively reduce feature dimensionality while still maintaining high classification accuracies.

C. Classification of Intended Movements in Stroke

Pattern-recognition analysis was performed using different feature sets and classifiers, with the optimal number of PCs previously determined. Table III summarizes the user-specific classification accuracies for all 20 intended upper-limb movements. High-average classification accuracies above 95% can

TABLE III
PATTERN-RECOGNITION RESULTS (MEAN ± SD) IN STROKE SUBJECTS, AVERAGED ACROSS FIVEFOLD TESTS FOR EACH SUBJECT (UNIT: %)

Subject #	TD feature set			AR+RMS feature set		
	LDC	GMM	SVM	LDC	GMM	SVM
1	89.71 ± 7.93	93.53 ± 5.30	92.47 ± 7.51	90.41 ± 6.89	94.07 ± 4.34	93.44 ± 5.56
2	79.69 ± 16.76	83.96 ± 12.22	86.78 ± 11.77	80.42 ± 12.80	84.56 ± 11.36	85.22 ± 12.58
3	95.43 ± 2.22	97.29 ± 2.20	98.11 ± 1.40	94.93 ± 2.36	97.29 ± 2.20	98.14 ± 1.26
4	86.99 ± 5.34	89.06 ± 8.47	90.13 ± 5.40	87.50 ± 7.06	89.43 ± 9.22	91.22 ± 7.00
5	96.44 ± 3.03	96.33 ± 3.72	96.96 ± 3.73	93.55 ± 5.00	92.49 ± 3.10	94.86 ± 4.25
6	94.94 ± 2.35	95.40 ± 2.94	96.76 ± 1.65	95.45 ± 2.22	96.69 ± 2.36	96.33 ± 2.24
7	99.19 ± 1.56	99.19 ± 1.56	99.46 ± 1.20	99.87 ± 0.30	99.82 ± 0.40	99.87 ± 0.30
8	99.65 ± 0.56	99.83 ± 0.18	99.91 ± 0.12	99.43 ± 0.64	98.35 ± 2.18	99.82 ± 0.24
9	91.86 ± 7.50	94.35 ± 3.02	94.70 ± 4.67	94.14 ± 4.04	95.52 ± 2.86	95.07 ± 3.55
10	97.57 ± 1.67	98.51 ± 2.48	98.38 ± 2.28	97.97 ± 2.60	98.52 ± 2.09	98.21 ± 2.10
11	98.57 ± 2.09	98.75 ± 2.32	99.78 ± 0.23	99.02 ± 0.92	98.35 ± 2.27	99.46 ± 0.44
12	98.63 ± 3.06	99.06 ± 1.99	99.74 ± 0.57	98.42 ± 2.97	99.28 ± 1.01	98.98 ± 1.76
Overall	**94.05 ± 6.02**	**95.44 ± 4.75**	**96.10 ± 4.27**	**94.26 ± 5.77**	**95.36 ± 4.58**	**95.88 ± 4.34**

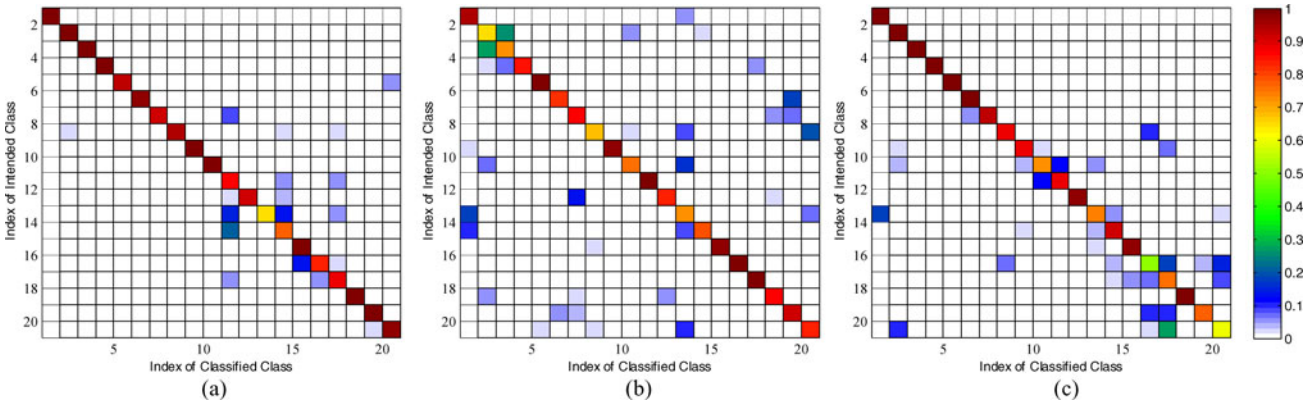

Fig. 5. Pseudocolor plots of confusion matrices derived from the classification results of three subjects: (a) Subject 1, (b) Subject 2, and (c) Subject 4, using the TD feature set and the SVM classifier. The results in confusion matrices are averaged across fivefold cross-validation and expressed as percentages. In each confusion matrix, the main diagonal elements represent the percentages of correct classifications (accuracy) for each class and others are error rates.

be achieved for most subjects, except for Subject 1, Subject 2, and Subject 4.

Across all subjects, there was no significant difference in the accuracy of the TD versus AR+RMS feature sets ($p = 0.57$, $p = 0.86$, and $p = 0.45$, with LDC, GMM and SVM, respectively). But the TD feature set has better computational efficiency due to it lower feature dimension, as compared with the AR+RMS feature set. In the examination of the three different classifiers, we found that with the TD or AR+RMS feature set, the GMM, and SVM classifiers achieved slightly higher accuracies than the LDC classifier (with TD feature set: $p = 0.009$ for GMM versus LDC, $p = 0.003$ for SVM versus LDC; with AR+RMS feature set: $p = 0.048$ for GMM versus LDC and $p = 0.005$ for SVM versus LDC). It was also observed that when using the TD feature set, the SVM classifier exhibits the best performance for most of the subjects with an average improvement of approximately 0.66% and 2.05%, as compared with the GMM ($p = 0.033$) and LDC ($p = 0.003$) classifiers, respectively. The highest classification accuracy of 96.10 ± 4.27% was achieved using the TD feature set and the SVM classifier.

Fig. 5 shows pseudocolor plots of the confusion matrices to present the class-to-class results of three subjects: Subject 1, Subject 2, and Subject 4, for whom the classification accuracies were below 95%. Examination of their average class-to-class results revealed that the majority of misclassifications were related to a few classes. For example, for Subject 1 and Subject 4, intended movements regarding finger functions were confused

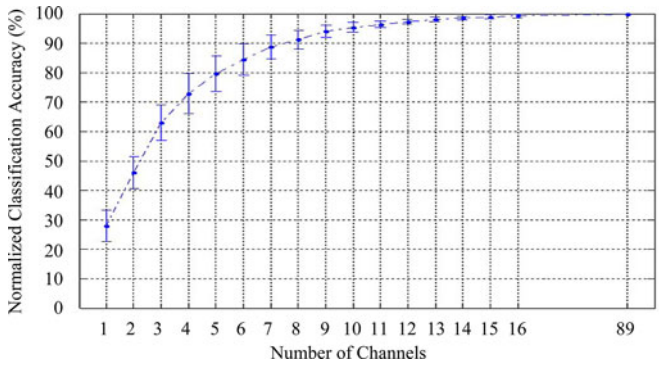

Fig. 6. Normalized classification accuracies from all 12 stroke subjects as a function of number of channels. For each subject, the classification accuracies were averaged across fivefold cross-validation tests and then normalized to his/her maximum accuracy using all 89 channels. The normalized accuracies across all subjects were averaged and plotted with SD error bars. TD feature set and SVM classifier were used for classification of all 20 functional movements.

with each other. For Subject 2, some intended wrist movements were not identified.

D. Preliminary Channel Selection Analysis

The preliminary channel selection analysis indicated that it was feasible to greatly reduce the number of EMG channels while maintaining high classification accuracy. As shown in Fig. 6, on average, eight selected channels can maintain 90% of the maximum accuracy achieved with all the 89 channels.

IV. Discussions and Conclusion

In the current study, we have demonstrated that applying pattern-recognition techniques to high-density surface EMG recordings achieved high accuracies in classification of 20 intended movements involving the affected limb of the stroke subjects. The detectable movement intentions can be used as a trigger signal for EMG-driven therapy or assistive devices. Voluntary user interactions are important to promote the currently available robot-aided therapy for stroke patients to improve motor abilities [14], [44]. The identified tasks can also be incorporated with myoelectric control devices to enable stroke subjects to voluntarily perform fundamental functional tasks.

In a previous study using untargeted placement of a limited number (10) of electrodes [2], relatively low accuracies were achieved for classification of six functional hand movements. It was reported that the classification accuracy was associated with the subject's functional impairment level, as manifested by the subject's Chedoke–McMaster scale. For example, the mean classification accuracy was 71.3% for moderately impaired subjects (Chedoke Stage of Hands 4 and 5) and 37.9% for severely impaired subjects (Chedoke Stage of Hands 2 and 3). By contrast, with the high-density surface recording and pattern-recognition analysis, high accuracies (approximately 95%) were achieved in classification of 20 different arm, hand, and finger/thumb movements involving the affected limb of the stroke subjects. The high accuracy was consistent across different subjects who had various levels of functional impairment (Chedoke–McMaster scale 2–5, Fugl–Meyer score 15–58).

Consistent with the previous findings [2], we also observed that classification performance was affected by the functional impairment level. Among all stroke subjects, the three accuracies below 95% were found in Subject 1 ($94.07 \pm 4.34\%$), Subject 2 ($86.78 \pm 11.77\%$), and Subject 4 ($91.11 \pm 7.00\%$). These three subjects demonstrated relatively low Chedoke–McMaster scales (two for all three subjects) and Fugl–Meyer scores (28 for Subject 1, 15 for Subject 2, and 19 for Subject 4). All of the rest subjects achieved classification accuracies above 95%. It is worth noting the rest subjects had varying impairment levels (Chedoke-McMaster scale range: 2–5; Fugl-Meyer score range: 20–58), demonstrating the advantages of the high-density EMG recording over the untargeted placement of a limited number of surface electrodes. Furthermore, a preliminary channel selection analysis indicates that it was possible to maintain high levels of classification accuracy with only a few electrodes. Thus, high-density EMG can be used to optimize electrode selection to facilitate clinical application of the myoelectric pattern-recognition techniques.

Across all subjects, there was no appreciable difference in the classification accuracy of the TD versus AR+RMS feature sets. All the three classifiers showed high accuracies in classification of the 20 different motions in stroke. This confirms the previous findings that the LDC, does not compromise classification accuracy in EMG pattern recognition, compared with the more complex and potentially powerful classifiers [25], [26], [32]. Besides, the LDC is much simpler to implement and much faster to train; thus, it is frequently used in myoelectric control. Our analysis also indicated that the SVM classifier achieved the highest overall classification accuracies, especially when less number of PCs were used. The GMM classifier also achieved slightly higher ($<1.5\%$) overall classification accuracy than the LDC (see Table III). The slight performance improvement of the SVM and GMM classifiers may be due to several construction advantages, such as the good generalization to novel data [39], [40] for the SVM classifier and the combination of mixture Gaussian densities [31], [36] for the GMM classifier.

Similar to myoelectric prosthesis control, the ability to proportionally control velocity or force of assistive device components significantly enhances function [3]. In our experiments, subjects were asked to maintain a moderate constant force, and feedback regarding the level of contraction was not provided; thus, the results do not specifically address whether proportional control is possible in stroke subjects using pattern-recognition techniques. On inspection of the data of this study, it is evident that the contraction levels do vary, suggesting that proportional control may be possible. Further experiments are necessary to determine the dynamic range of contraction levels that is possible, without significantly degrading classifier performance.

Compared with myoelectric prosthesis control, there are also many factors that are unique to stoke rehabilitation. For example, it is likely that the voluntary EMG activities are contaminated by the involuntary muscle contractions as a result of muscle spasticity. In this study and the previous one as well [2], additional rest periods were allowed for stroke subjects to decrease the muscle spasticity or involuntary EMG activities. A previous study has shown that the classification performance may not be compromised as long as the interference is consistently present in specific channels for all the tested classes [45]. It is presently unclear how relatively high levels of muscle spasticity may affect the classification performance. Further experimental study is underway to compare the classification performance in presence or absence of strong muscle spasticity. In addition to classification accuracy, involuntary EMG activity may also compromise the muscle activity onset detection using conventional amplitude threshold based methods. Thus, development of appropriate signal parameters is required to facilitate automatic onset or offset detection for each voluntary task. One promising approach is to process the signal in the nonlinear dynamic or complexity domain. For example, our pilot study has shown that the voluntary EMG bursts can be distinguished from spontaneous tonic spikes based on approximate entropy measurements [46].

Finally, it should be emphasized that the EMG activity is subject-specific for stroke survivors. This can be demonstrated from the distinct EMG contour plots for the same movement of different stroke subjects (see Fig. 3), as well as the inconsistent class-to-class classification errors among different stroke subjects. The subject-specific EMG activity may be due to different neurological and functional impairment levels for the stroke subjects. The variance in daily activity and therapeutic interventions may also contribute to the different EMG patterns. The subject-specific EMG activity and classification performance suggest that the myoelectric pattern-recognition control system should be individually customized for stroke survivors. The design should consider the motor control characteristics of each specific subject. The selection of target tasks should also reflect the functional impairment level and meet the need of each individual subject.

In conclusion, this study presents a novel framework using high-density surface EMG recording and pattern-recognition analysis for stroke survivors. High accuracies can be obtained in classification of 20 arm, hand, finger/thumb movements involving the affected limb, suggesting that with myoelectric pattern-recognition techniques substantial motor control information can be extracted from the paretic muscles of stroke subjects. Such information will potentially enable volitional control of assistive devices, thereby facilitating the functional restoration for the affected limb. Our future work will concentrate on challenges toward implementing a practical myoelectric control system toward improved stroke rehabilitation. These include minimizing electrode numbers, determining acceptable electrode locations, optimizing electrode recording configurations, and dealing with the challenges of the EMG recording in a dynamic environment. In addition, assessment of other signal-recording approaches (e.g., implanted myoelectric sensors [47]) and decoding schemes (e.g., blind source separation [48]) may provide further useful information.

REFERENCES

[1] J. Mackay and G. A. Mensah. (2004). *The Atlas of Heart Disease and Stroke*. Geneva, Switzerland: World Health Organization. (2004). [Online]. Available: http://www.who.int/cardiovascular_diseases/resources/atlas/en/

[2] S. W. Lee, K. M. Wilson, B. A. Lock, and D. G. Kamper, "Subject-specific myoelectric pattern classification of functional hand movements for stroke survivors," *IEEE Trans. Neural Syst. Rehabil. Eng.*, vol. 19, no. 5, pp. 558–566, Oct. 2011.

[3] R. Song, K. Tong, X. Hu, and L. Li, "Assistive control system using continuous myoelectric signal in robot-aided arm training for patients after stroke," *IEEE Trans. Neural Syst. Rehabil. Eng.*, vol. 16, no. 4, pp. 371–379, Aug. 2008.

[4] H. I. Krebs, B. T. Volpe, D. Williams, J. Celestino, S. K. Charles, D. Lynch, and N. Hogan, "Robot-aided neurorehabilitation: A robot for wrist rehabilitation," *IEEE Trans. Neural Syst. Rehabil. Eng.*, vol. 15, no. 3, pp. 327–335, Sep. 2007.

[5] L. Dipietro, H. I. Krebs, S. E. Fasoli, B. T. Volpe, J. Stein, C. Bever, and N. Hogan, "Changing motor synergies in chronic stroke," *J. Neurophysiol.*, vol. 98, no. 2, pp. 757–768, Aug. 2007.

[6] P. S. Lum, C. G. Burgar, and P. C. Shor, "Evidence for improved muscle activation patterns after retraining of reaching movements with the MIME robotic system in subjects with post-stroke hemiparesis," *IEEE Trans. Neural Syst. Rehabil. Eng.*, vol. 12, no. 2, pp. 186–194, Jun. 2004.

[7] P. S. Lum, C. G. Burgar, D. E. Kenney, and H. F. Van der Loos, "Quantification of force abnormalities during passive and active-assisted upper-limb reaching movements in post-stroke hemiparesis," *IEEE Trans. Biomed. Eng.*, vol. 46, no. 6, pp. 652–662, Jun. 1999.

[8] J. Liepert, H. Bauder, H. R. Wolfgang, W. H. Miltner, E. Taub, and C. Weiller, "Treatment-induced cortical reorganization after stroke in humans," *Stroke*, vol. 31, no. 6, pp. 1210–1216, Jun. 2000.

[9] C. E. Levy, D. S. Nichols, P. M. Schmalbrock, P. Keller, and D. W. Chakeres, "Functional MRI evidence of cortical reorganization in upper-limb stroke hemiplegia treated with constraint-induced movement therapy," *Am. J. Phys. Med. Rehabil.*, vol. 80, no. 1, pp. 4–12, Jan. 2001.

[10] G. Nelles, W. Jentzen, M. Jueptner, S. Müller, and H. C. Diener, "Arm training induced brain plasticity in stroke studied with serial positron emission tomography," *Neuroimage*, vol. 13, no. 6, pp. 1146–1154, Jun. 2001.

[11] L. Dipietro, M. Ferraro, J. J. Palazzolo, H. I. Krebs, B. T. Volpe, and N. Hogan, "Customized interactive robotic treatment for stroke: EMG-triggered therapy," *IEEE Trans. Neural Syst. Rehabil. Eng.*, vol. 13, no. 3, pp. 325–334, Sep. 2005.

[12] J. A. Cozens, "Robotic assistance of an active upper limb exercise in neurologically impaired patients," *IEEE Trans. Rehabil. Eng.*, vol. 7, no. 2, pp. 254–256, Jun. 1999.

[13] X. L. Hu, K. Y. Tong, R. Song, X. J. Zheng, K. H. Lui, W. W. Leung, S. Ng, and S. S. Au-Yeung, "Quantitative evaluation of motor functional recovery process in chronic stroke patients during robot-assisted wrist training," *J Electromyogr. Kinesiol.*, vol. 19, no. 4, pp. 639–650, Aug. 2009.

[14] X. L. Hu, K. Y. Tong, R. Song, X. J. Zheng, and W. W. Leung, "A comparison between electromyography-driven robot and passive motion device on wrist rehabilitation for chronic stroke," *Neurorehabil. Neural Repair*, vol. 23, no. 8, pp. 837–846, Oct. 2009.

[15] R. P. Van Peppen, G. Kwakkel, S. Wood-Dauphinee, H. J. Hendriks, P. J. Van der Wees, and J. Dekker, "The impact of physical therapy on functional outcomes after stroke: What's the evidence?" *Clin. Rehabil.*, vol. 18, no. 8, pp. 833–862, Dec. 2004.

[16] J. W. Krakauer, "Motor learning: Its relevance to stroke recovery and neurorehabilitation," *Curr. Opin. Neurol.*, vol. 19, no. 1, pp. 84–90, Feb. 2006.

[17] M. A. Oskoei and H. Hu, "Myoelectric control systems—A survey," *Biomed. Signal Process. Control*, vol. 2, no. 4, pp. 275–294, Oct. 2007.

[18] C. Fleischer, A. Wege, K. Kondak, and G. Hommel, "Application of EMG signals for controlling exoskeleton robots," *Biomed Tech (Berl)*, vol. 51, no. 5–6, pp. 314–319, Dec. 2006.

[19] J. Stein, K. Narendran, J. McBean, K. Krebs, and R. Hughes, "Electromyography controlled exoskeletal upper-limb–powered orthosis for exercise training after stroke," *Am. J. Phys. Med. Rehabil.*, vol. 86, pp. 255–261, Apr. 2007.

[20] N. S. Ho, K. Y. Tong, X. L. Hu, K. L. Fung, X. J. Wei, W. Rong, and E. A. Susanto, "An EMG-driven exoskeleton hand robotic training device on chronic stroke subjects: Task training system for stroke rehabilitation," in *Proc. IEEE Int. Conf. Rehabil. Robot.*, Jun. 2011, pp. 1–5.

[21] L. J. Hargrove, E. J. Scheme, K. B. Englehart, and B. S. Hudgins, "Multiple binary classifications via linear discriminant analysis for improved controllability of a powered prosthesis," *IEEE Trans. Neural. Syst. Rehabil. Eng.*, vol. 18, no. 1, pp. 49–57, Feb. 2010.

[22] Z. Ke, S. P. Yip, L. Li, X. X. Zheng, and K. Y. Tong, "The effects of voluntary, involuntary, and forced exercises on brain-derived neurotrophic factor and motor function recovery: A rat brain ischemia model," *PLoS One*, vol. 6, no. 2, e16643 (pp. 1–8), Feb. 2011.

[23] A. R. Fugl-Meyer, L. Jaasko, I. Leyman, S. Olsson, and S. Steglind, "The post-stroke hemiplegic patient—1. A method for evaluation of physical performance," *Scand. J. Rehabil. Med.*, vol. 7, pp. 13–31, 1975.

[24] C. A. Gowland, "Staging motor impairment after stroke," *Stroke*, vol. 21, (Suppl. II), pp. 19–21, Sep. 1990.

[25] P. Zhou, M. M. Lowery, K. B. Englehart, H. Huang, G. Li, L. Hargrove, J. P. Dewald, and T. A. Kuiken, "Decoding a new neural machine interface for control of artificial limbs," *J Neurophysiol.*, vol. 98, no. 5, pp. 2974–2982, Nov. 2007.

[26] P. Zhou, N. L. Suresh, and W. Z. Rymer, "Surface electromyogram analysis of the direction of isometric torque generation by the first dorsal interosseous muscle," *J. Neural Eng.*, vol. 8, no. 3, 036028 (pp. 1–10), Jun. 2011.

[27] X. Zhang, X. Chen, Y. Li, V. Lantz, K. Wang, and J. Yang, "A Framework for Hand Gesture Recognition Based on Accelerometer and EMG

Sensors," *IEEE Trans. Syst. Man Cybern, A: Syst. Humans*, vol. 41, no. 6, pp. 1064–1076, Nov. 2011.
[28] B. Hudgins, P. A. Parker, and R. Scott, "A new strategy for multifunction myoelectric control," *IEEE Trans. Biomed. Eng.*, vol. 40, no. 1, pp. 82–94, Jan. 1993.
[29] D. Farina and R. Merletti, "Comparison of algorithms for estimation of EMG variables during voluntary isometric contractions," *J. Electromyogr. Kinesiol.*, vol. 10, no. 5, pp. 337–349, Oct. 2000.
[30] K. Englehart and B. Hudgins, "A robust, real-time control scheme for multifunction myoelectric control," *IEEE Trans. Biomed. Eng.*, vol. 50, no. 7, pp. 848–854, Jul. 2003.
[31] Y. Huang, K. B. Englehart, B. Hudgins, and A. D. Chan, "A Gaussian mixture model based classification scheme for myoelectric control of powered upper limb prostheses," *IEEE Trans. Biomed. Eng.*, vol. 52, no. 11, pp. 1801–1811, Nov. 2005.
[32] L. J. Hargrove, K. Englehart, and B. Hudgins, "A comparison of surface and intramuscular myoelectric signal classification," *IEEE Trans Biomed Eng.*, vol. 54, no. 5, pp. 847–853, May. 2007.
[33] C. Liu and H. Wechsler, "Robust coding schemes for indexing and retrieval from large face databases," *IEEE Trans. Image Process.*, vol. 9, no. 1, pp. 132–137, Jan. 2000.
[34] R. O. Duda, P. E. Hart, and D. G. Stork, *Pattern Classification*, 2nd ed. New York: Wiley, 2001.
[35] J. Yang and J. Yang, "Why can LDA be performed in PCA transformed space?" *Pattern Recog.*, vol. 36, no. 2, pp. 563–566, Feb. 2003.
[36] D. A. Reynolds and R. C. Rose, "Robust text-independent speaker identification using Gaussian mixture speaker models," *IEEE Trans. Speech Audio Process.*, vol. 3, no. 1, pp. 72–83, Jan. 1995.
[37] D. A. Reynolds, "An overview of automatic speaker recognition technology," in *Proc. Int. Conf. Acoust., Speech, Signal Process.*, vol. 4, Orlando, FL, May 2002, pp. 4072–4075.
[38] A. S. Malegaonkar, A. M. Ariyaeeinia, and P. Sivakumaran, "Efficient speaker change detection using adapted gaussian mixture models," *IEEE Trans. Speech Audio Process.*, vol. 15, no. 6, pp. 1859–1869, Aug. 2007.
[39] M. A. Oskoei and H. Hu, "Support vector machine-based classification scheme for myoelectric control applied to upper limb," *IEEE Trans. Biomed. Eng.*, vol. 55, no. 8, pp. 1956–1965, Aug. 2008.
[40] C. Chang and C. Lin, "LIBSVM: a library for support vector machines," *ACM Trans. Intell. Syst. Technol.*, vol. 2, no. 3, pp. 27:1–27: 27, Apr. 2011. Software available at http://www.csie.ntu.edu.tw/∼cjlin/libsvm
[41] H. Huang, P. Zhou, G. Li, and T. A. Kuiken, "An analysis of EMG electrode configuration for targeted muscle reinnervation based neural machine interface," *IEEE Trans. Neural Syst. Rehabil. Eng.*, vol. 16, no. 1, pp. 37–45, Feb. 2008.
[42] H. Huang, P. Zhou, G. Li, and T. A. Kuiken, "Spatial filtering improves EMG classification accuracy following targeted muscle reinnervation," *Ann. Biomed. Eng.*, vol. 37, no. 9, pp. 1849–1857, Sep. 2009.
[43] P. Somol, P. Pudil, J. Novovicova, and P. Paclik, "Adaptive floating search methods in feature selection," *Pattern Recognit. Lett.*, vol. 20, no. 11–13, pp. 1157–1163, Nov. 1999.
[44] J. Cauraugh, K. Light, S. Kim, M. Thigpen, and A. Behrman, "Chronic motor dysfunction after stroke: Recovering wrist and finger extension by electromyography-triggered neuromuscular stimulation," *Stroke*, vol. 31, no. 6, pp. 1360–1364, Jun. 2000.
[45] L. Hargrove, P. Zhou, K. Englehart, and T. A. Kuiken, "The effect of ECG interference on pattern-recognition-based myoelectric control for targeted muscle reinnervated patients," *IEEE Trans. Biomed. Eng.*, vol. 56, no. 9, pp. 2197–2201, Sep. 2009.
[46] P. Zhou, P. E. Barkhaus, X. Zhang, and W. Z. Rymer, "Characterizing the complexity of spontaneous motor unit patterns of amyotrophic lateral sclerosis using approximate entropy," *J. Neural Eng.*, vol. 8, no. 6, 066010 (pp. 1–10), Dec. 2011.
[47] G. E. Loeb, R. A. Peck, W. H. Moore, and K. Hook, "BION^{TM} system for distributed neural prosthetic interfaces," *Med. Eng. Phys.*, vol. 23, pp. 9–18, Jan. 2001.
[48] D. Farina, C. Fevotte, C. Doncarli, and R. Merletti, "Blind separation of linear instantaneous mixtures of non-stationary surface myoelectric signals," *IEEE Trans. Biomed. Eng.*, vol. 51, no. 9, pp. 1555–1567, Sep. 2004.

Xu Zhang (M'11) received the B.S. degree in electronic information science and technology and the Ph.D. degree in biomedical engineering from University of Science and Technology of China, Hefei, China, in 2005 and 2010, respectively.

He is currently a Postdoctoral Fellow at the Rehabilitation Institute of Chicago, Chicago, IL. His research interests include biomedical signal processing, pattern recognition, and neurorehabilitation engineering.

Ping Zhou (S'01–M'05–SM'07) received the B.S. degree in electrical engineering and the M.S. degree in biomedical engineering from the University of Science and Technology of China, Hefei, China, in 1995 and 1999, respectively, and the Ph.D. degree in biomedical engineering from Northwestern University, Evanston, IL, in 2004. His Ph.D. dissertation project was performed as part of the Sensory Motor Performance Program (SMPP), Rehabilitation Institute of Chicago, Chicago, IL.

From 2004 to 2006, he was a Research Associate in the Neural Engineering Center for Artificial Limbs (NECAL), Rehabilitation Institute of Chicago. After that he was a Research Scientist in NECAL and later in SMPP, Rehabilitation Institute of Chicago. He has been an Adjunct Assistant Professor since 2006 in the Department of Physical Medicine and Rehabilitation, Northwestern University, Chicago, and a Professor since 2012 in the Institute of Biomedical Engineering, University of Science and Technology of China. His current research interests include biomedical signal (in particular, EMG) processing, spinal motor neuron/motor unit pathophysiology in neurologic disorders, noninvasive electrodiagnosis of neuromuscular diseases, computational modeling of neuromuscular systems, myoelectric prosthesis control, and assistive devices.